ORGANOMETALLICS
Article

Organometallics **2010,** *29,* 1551–1559 1551
DOI: 10.1021/om900852y

Zirconium Complexes of Symmetric and of Chiral Diketiminate Ligands: Synthesis, Crystal Structures, and Reactivities

Ibrahim El-Zoghbi, Saïda Latreche, and Frank Schaper*

Département de Chimie, Université de Montréal, Montréal, Québec, H3C 3J7, Canada

Received October 1, 2009

Reaction of *N*,*N*-dialkyl-2-amino-4-iminopent-2-enes (*nacnac*^{R}H; R = Bn (**1a**), Cy (**1b**), *R*-CH(Me)Ph (**1c**)) with *n*BuLi afforded the lithium salts *nacnac*^{R}Li(THF), **2a**−**c**. Further reaction with $ZrCl_4$ or $ZrCl_4(THF)_2$ yielded the *cis*-dichloride complexes *nacnac*$^{R}{}_2ZrCl_2$, **3a**−**c**. As a side reaction in the synthesis of **3c**, CH activation of CH(Me)Ph under formal HCl elimination was observed. Complex **3a** could also be obtained by reaction of *nacnac*^{Bn}H with nBu_2ZrCl_2. *nacnac*$^{Bn}{}_2ZrMe_2$, **5**, was formed in reactions of **3a** with MeLi in the presence of excess $AlMe_3$ and was isolated from the reaction of Me_2ZrCl_2 with **2a**. Complex **5** reacts with aluminum chloride compounds, but not with lithium chloride, to form the dichloride complex **3a** and with ethanol to form *nacnac*$^{Bn}{}_2Zr(OEt)_2$, **6**. X-ray diffraction studies have been performed for **3a**−**c**, **5**, and **6**.

Introduction

β-Diketiminate ("*nacnac*") ligands have gained increasing popularity since the mid 1990s due to their suitability as spectator ligands.[1] Zirconium complexes with diketiminate ligands (based on 2,4-diiminopentane)[2,3] appeared in the literature in 1994 with the work of Lappert and co-workers,[4] followed by more extensive work in the groups of Collins,[5,6] Smith,[7,8] Novak,[9] and others.[10−16] Interest in these complexes was focused mostly on their application in olefin, notably ethylene, polymerization[5,9−11] or on investigations of the ligand coordination mode,[4,6−8,15,16] which varies between in-plane κ^2-coordination and out-of-plane $\eta^{4/5}$-coordination. With a single exception,[12] ligands with aryl substituents on nitrogen were employed, as is the case in most diketiminate metal complexes. Variations in the ligand framework were limited by the fact that *ortho*-substitution of both *N*-aryl substituents impedes the coordination of a second diketiminate ligand to zirconium,[6−8] although the use of unsymmetrical ligands allowed the substitution of at least one phenyl ring.[11] Complexation of the bulky bis(trimethylsilyl) diketiminate (*nacnac*^{TMS}) to Zr resulted in a rearrangement of one *nacnac*^{TMS} ligand.[10] Coordination of two diketiminate ligands to a ZrX_2 fragment should favor the formation of C_2-symmetric *cis*-complexes, with two homotopic Zr−X sites, whose environment is strongly influenced by the substituent on nitrogen. We present in the following the syntheses of zirconium bis(diketiminate) complexes with aliphatic substituents on nitrogen, which increase the possibilities of steric variations in these complexes and allow easy introduction of chirality, the investigation of their solid state and solution structures, and (attempted) applications in catalysis.

Results and Discussion

***nacnac*$_2$ZrCl$_2$ Complexes.** Diketimine ligands **1a**−**c** were obtained from condensation of acetylacetone and the respective amine in the presence of stoichiometric amounts of *para*-toluenesulfonic acid. Synthesis of **1a** and **1c** by this method has been previously described.[17,18] Ligand **1b** has been prepared previously using $TiCl_4$ as an activator in 29% yield.[19] Deprotonation with *n*BuLi in THF yielded the THF-coordinated lithium salts **2a**−**c**, which were used without

*Corresponding author. E-mail: Frank.Schaper@umontreal.ca.

(1) Bourget-Merle, L.; Lappert, M. F.; Severn, J. R. *Chem. Rev.* **2002**, *102*, 3031.
(2) For other structures, for example incorporating a pyridyl moiety, see: Deelman, B.-J.; Hitchcock, P. B.; Lappert, M. F.; Leung, W.-P.; Lee, H.-K.; Mak, T. C. W. *Organometallics* **1999**, *18*, 1444.
(3) Cortright, S. B.; Huffman, J. C.; Yoder, R. A.; Coalter, J. N.; Johnston, J. N. *Organometallics* **2004**, *23*, 2238.
(4) Hitchcock, P. B.; Lappert, M. F.; Liu, D.-S. *Chem. Commun.* **1994**, 2637.
(5) Vollmerhaus, R.; Rahim, M.; Tomaszewski, R.; Xin, S.; Taylor, N. J.; Collins, S. *Organometallics* **2000**, *19*, 2161.
(6) Rahim, M.; Taylor, N. J.; Xin, S.; Collins, S. *Organometallics* **1998**, *17*, 1315.
(7) Kakaliou, L.; Scanlon, W. J.; Qian, B.; Baek, S. W.; Smith, M. R.; Motry, D. H. *Inorg. Chem.* **1999**, *38*, 5964.
(8) Qian, B.; Scanlon, W. J.; Smith, M. R.; Motry, D. H. *Organometallics* **1999**, *18*, 1693.
(9) Jin, X.; Novak, B. M. *Macromolecules* **2000**, *33*, 6205. Novak, B. M.; Jin, X.; Tanaka, H. *Polym. Prepr.* (*Am. Chem. Soc., Div. Polym. Chem.*) **2000**, *41*, 399.
(10) Shaviv, E.; Botoshansky, M.; Eisen, M. S. *J. Organomet. Chem.* **2003**, *683*, 165.
(11) Gong, S.; Ma, H.; Huang, J. *J. Organomet. Chem.* **2008**, *693*, 3509.
(12) Franceschini, P. L.; Morstein, M.; Berke, H.; Schmalle, H. W. *Inorg. Chem.* **2003**, *42*, 7273.
(13) Basuli, F.; Kilgore, U. J.; Brown, D.; Huffman, J. C.; Mindiola, D. J. *Organometallics* **2004**, *23*, 6166.
(14) Hamaki, H.; Takeda, N.; Tokitoh, N. *Organometallics* **2006**, *25*, 2457.
(15) Fortuné, R.-V.; Verguet, E.; Oguadinma, P. O.; Schaper, F. *Acta Crystallogr.* **2007**, *E63*, m2822.
(16) Verguet, E.; Fortuné, R.-V.; Oguadinma, P. O.; Schaper, F. *Acta Crystallogr.* **2007**, *E63*, m2539. Verguet, E.; Oguadinma, P. O.; Schaper, F. *Acta Crystallogr.* **2007**, *E63*, m2541.
(17) Oguadinma, P. O.; Schaper, F. *Organometallics* **2009**, *28*, 4089.
(18) Oguadinma, P. O.; Schaper, F. *Organometallics* **2009**, *28*, 6721.
(19) Clegg, W.; Coles, S. J.; Cope, E. K.; Mair, F. S. *Angew. Chem., Int. Ed.* **1998**, *37*, 796.

Published on Web 02/26/2010

Scheme 1

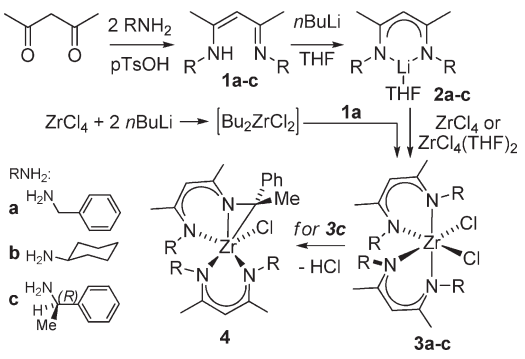

further purification (Scheme 1). Reaction of **2a**−**c** with $ZrCl_4$ or $ZrCl_4(THF)_2$ in toluene afforded the respective bis-(diketiminate) complexes *nacnac*$^{Bn}{}_2ZrCl_2$, **3a**, *nacnac*$^{Cy}{}_2$-$ZrCl_2$, **3b**, and (*R*,*R*-*nacnac*^{MeBn})$_2ZrCl_2$, **3c**, in moderate yields (Scheme 1). The choice of zirconium starting material or the solvent (toluene, THF) did not seem to influence reaction yields. Following an alternative synthetic route,[20] reaction of nBu$_2ZrCl_2$, generated *in situ* by reaction of nBuLi with $ZrCl_4$, with the neutral ligand **1a** in toluene at 90 °C improved the yield of **3a** from 35% to 75%. Similar reactions with **1b** and **1c** in toluene or hexane at various temperatures and reaction times led only to unidentified product mixtures, which did not contain **3b** or **3c** in significant amounts. Reactions of diketiminate ligands with secondary alkyl substituents on nitrogen seem to be too slow with respect to the instability of nBu$_2ZrCl_2$.

X-ray diffractions studies of complexes **3a**−**c** (Figures 1 and 2, Table 1) show distorted octahedral coordination geometries around the zirconium center (X−Zr−X angles of 78−107°). In all cases the expected *cis*-geometry of the $ZrCl_2$ fragment is found. Complexes **3a** and **3b** contain a crystallographic C_2-axis, while chiral complex **3c** crystallizes with two diastereomers in the asymmetric unit, which, however, approach C_2-symmetry. The structural features of **3a**−**c** seem to be governed by steric interactions between the alkyl substituent on nitrogen and the atoms coordinated to the metal center. The complex distorts in a way to place the N-substituent between two chloride ligands (or between chloride and nitrogen) instead of the eclipsed placement expected from an idealized geometry. Similar distortions were observed, sometimes to a lesser extent, in related octahedral bis(diketiminato) zirconium complexes,[6,7,12] while they are mostly absent in zirconium complexes with two aminoketone (*acnac*) ligands, where the oxygen atom occupies the position *trans* to the chloride (or amide) ligands.[7,12,21] For all complexes, the *N*-alkyl substituents are oriented away from the chloride ligands, indicating stronger steric interactions of the alkyl substituent with the chloride ligand than with the methyl group in the ligand backbone.

The diastereomeric Δ- and Λ-isomers of **3c** can both be found in the asymmetric unit. Changes in the Δ/Λ-conformation of the complex are accompanied by changes in the conformation of the diketiminate ligand. In the Δ-isomer, the diketiminate ligands retain a C_2-symmetric conformation with the phenyl substituents *anti* toward each other. In the Λ-isomer, rotation around the N1−C20 and N4−C50 bonds places the phenyl rings of each diketiminate in a *syn*-orientation, comparable to the C_s-symmetric ligand conformation observed in **3a** (Figure 1). Consequently, methyl groups C27 and C57 instead of hydrogen atoms are oriented toward the Zr center, causing an increased distortion from octahedral geometry, increased Zr1−Cl distances, and a reduced Cl1−Zr1−Cl2 angle in Λ-**3c** compared to Δ-**3c** (Table 1).

The zirconium atom in **3a**−**c** is bent significantly out of the mean plane of the ligand (bending angles of 34−49°, Table 1), as commonly observed in sterically encumbered diketiminate complexes.[1] Since the nitrogen atoms retain their planar geometry (e.g., for **3a**: $\sum$(X−N1−Y) = 359°, $\sum$(X−N2−Y) = 359°), the alkyl substituents on N are displaced out of the ligand mean plane (Figure 3). In all cases, the remaining ligand framework adopts a boat-like conformation, which reduces the distance between the electron-rich central carbon atom of the ligand backbone and the zirconium center.[4] In diketiminate Zr complexes with a $\eta^{4/5}$-coordinated *nacnac* ligand, distances of the metal center to the central carbon atom are less than 2.8 Å.[5−7,13,16] The rather longer respective distances in **3a**−**c** (3.1−3.3 Å) indicate, as expected for octahedral coordinated Zr complexes, the absence of significant coordinative interactions between Zr and the central carbon atom (C3 in Figure 3). Similar ligand conformations in *nacnac* Sc complexes have likewise been ascribed to steric origins.[22] Leaving aside potential p_N−d donation, diketiminate ligands in **3a**−**c** thus act as κ^2-coordinated, 4 e$^-$-donor ligands.

Yellow crystals of **3c** were consistently contaminated with a minor amount of red crystalline material, which could not be isolated in sufficient quantity for characterization. X-ray analysis identified the contamination as the CH-activation product **4** (Scheme 1, Figure 4). The complex is nonsymmetric and its geometry best described as distorted square pyramidal with N1 and C27 sharing the apical position (X−Zr−X angles (X = Cl1, N2−N4) = 84−89°, X−Zr−Y angles (Y = centroid N1/C27) = 96−112°). The two *nacnac* ligands are coordinated differently. The CH-activated ligand is planar with an *anti*-orientation of the phenyl rings and the Zr atom coordinated in the ligand mean plane. In the second ligand, Zr is found to be bent quite strongly (62°) out of the mean ligand plane. Zr−C distances to the ligand backbone are shorter than those in **3c** (**4**: 2.8−2.9 Å, **3c**: 3.0−3.3 Å), but still noticeably longer than those observed in $\eta^{4/5}$-coordinated *nacnac* ligands (2.5−2.8 Å).[5−7,13,16] The shortened Zr−C$_{nacnac}$ distances are thus most likely due to steric reasons, i.e., the increased out-of-plane bending of the Zr atom.

The formation of **4** as a result of formal HCl elimination was surprising and only observed as a side reaction during the preparation of **3c**. Treatment of complexes **3a**−**c** with excess (1−2 equiv) of bases such as NaOtBu, NEt_3, pyridine, $Na(NSiMe_3)_2$, or nBuLi showed no reaction (or decomposition upon heating).

Dynamic Behavior in Solution. NMR spectra of complexes **3a**−**c** indicate that the complexes do not retain their conformation in solution. The ^{1}H NMR spectrum of **3a** in $CDCl_3$ at room temperature displays two doublets for diastereotopic hydrogen atoms of the benzyl CH_2 groups,

(20) Eisch, J. J.; Owuor, F. A.; Otieno, P. O. *Organometallics* **2001**, *20*, 4132.

(21) Jones, D.; Roberts, A.; Cavell, K.; Keim, W.; Englert, U.; Skelton, B. W.; White, A. H. *J. Chem. Soc., Dalton Trans.* **1998**, 255.

(22) Hayes, P. G.; Piers, W. E.; Lee, L. W. M.; Knight, L. K.; Parvez, M.; Elsegood, M. R. J.; Clegg, W. *Organometallics* **2001**, *20*, 2533.

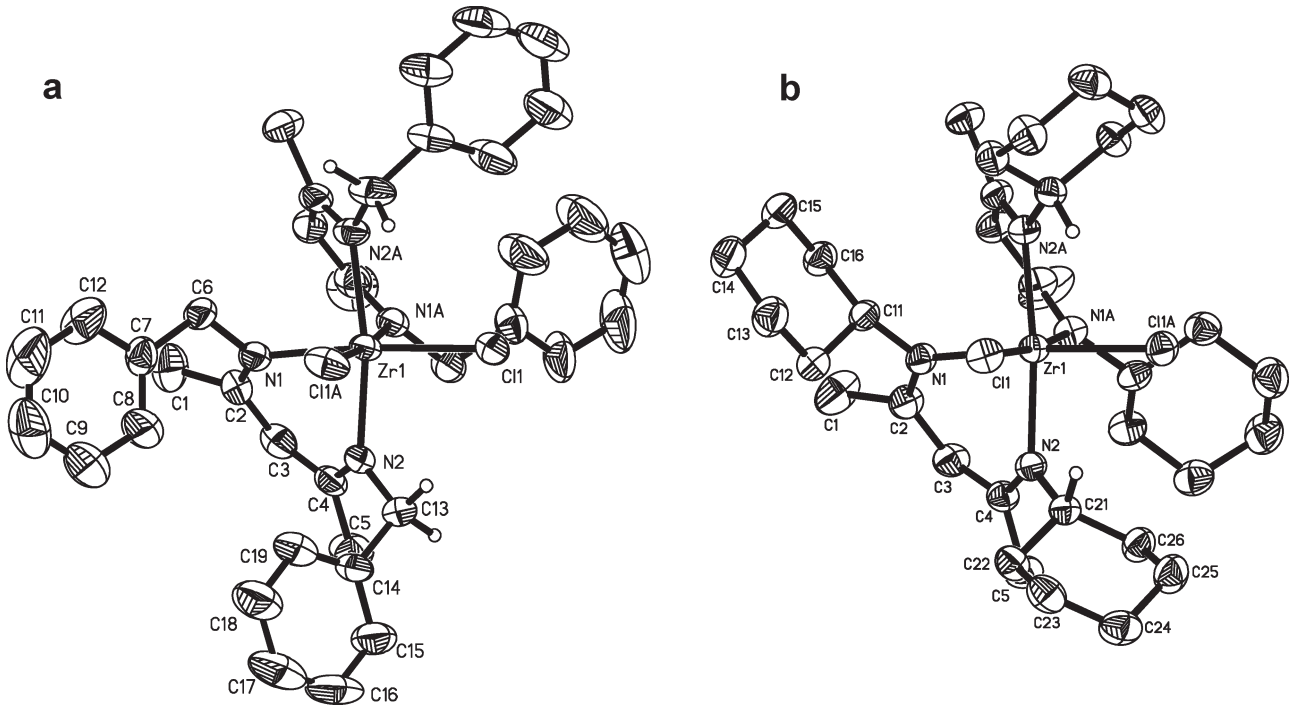

Figure 1. Crystal structures of **3a** and **3b**. Thermal ellipsoids are drawn at the 50% probability level. Most hydrogen atoms are omitted for clarity.

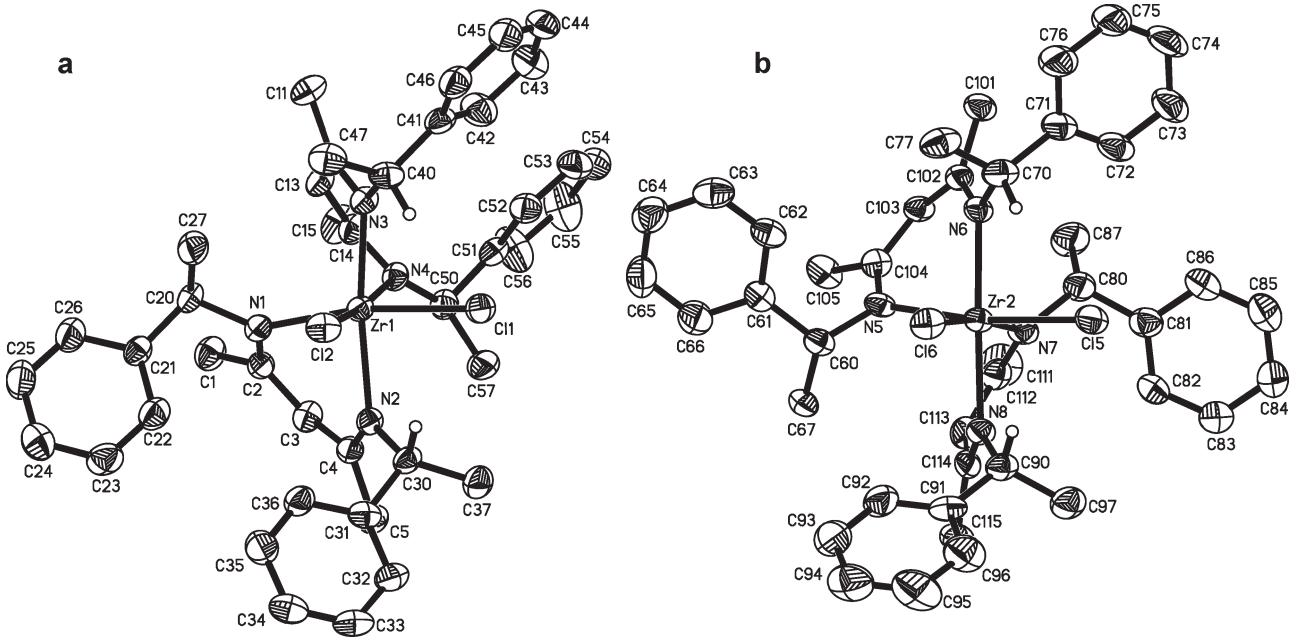

Figure 2. Crystal structures of Λ-**3c** (left) and Δ-**3c** (right), both found in the same asymmetric unit. Thermal ellipsoids are drawn at the 50% probability level. Most hydrogen atoms are omitted for clarity.

one singlet for the CH groups in the ligand backbone, and one singlet for the ligand methyl groups. Below −50 °C, four doublets for benzyl CH_2, two singlets for the methyl groups, but still only one sharp singlet for the backbone CH groups are obtained (Figure 5). The low-temperature spectrum is thus in agreement with the observed solid-state structure: a symmetric complex, in which unsymmetrically coordinated *nacnac* ligands are connected by a C_2-axis. The observed spectral changes on heating can be explained with an isomerization between the Δ- and Λ-enantiomer, which at the same time exchanges *trans* chloride and *trans* nitrogen sites (Scheme 2). Rahim et al. proposed a Bailar-twist mechanism for a similar fluxional behavior in *nacnac*$^{Ph}{}_2ZrCl_2$.[6] That two doublets are observed for the benzyl CH_2 group even at higher temperature indicates that the C_s-symmetric isomer with *trans* chloride ligands is not obtained, even as a short-lived intermediate at high temperatures.

The Bailar-twist is significantly slower for cyclohexyl-substituted **3b**, resulting in exchange-broadened peaks close to coalescence at room temperature. The presence of six signals for the cyclohexyl ring in ^{13}C spectra of **3b** at higher temperatures again indicates that isomerization occurs

Table 1. Selected Bond Distances [Å] and Bond Angles [deg] for 3a−c, 5, and 6[a]

	3a	3b	Λ-3c	Δ-3c	5	6
Zr−N1[b]	2.201(3)	2.235(2)	2.181(2) and 2.205(2)	2.177(3) and 2.183(2)	2.203(3) and 2.217(3)	2.288(2)−2.305(2)
Zr−N2[c]	2.190(2)	2.197(2)	2.213(3) and 2.246(3)	2.221(3) and 2.247(3)	2.289(3) and 2.295(3)	2.225(2)−2.232(2)
Zr−X[d]	2.455(1)	2.483(1)	2.499(1) and 2.516(1)	2.483(1) and 2.487(1)	2.290(4) and 2.297(4)	1.939(2)−1.954(2)
N1−C2/N2−C4	1.325(4) and 1.339(4)	1.339(3) and 1.331(2)	1.321(4)−1.357(4)	1.328(4)−1.348(4)	1.328(5)−1.338(5)	1.314(3)−1.336(3)
C2−C3/C3−C4	1.410(5) and 1.388(5)	1.397(3) and 1.410(3)	1.394(5)−1.408(4)	1.398(4)−1.413(4)	1.380(6)−1.403(5)	1.388(4)−1.416(4)
complex bending[e]	37	34	47−49	36−42	31	32−34
N1−Zr−N2[f]	78.06(9)	80.52(6)	83.71(9) and 85.46(9)	82.28(9) and 82.44(9)	74.56(11) and 74.81(11)	76.65(7)−77.52(8)
N−Zr−N[g]	86.71(13)−87.28(9)	86.7(1)−89.2(1)	91.32(9)−106.81(9)	91.31(9)−98.60(9)	77.31(11)−127.20(12)	83.20(7)−87.37(8)
X1−Zr−X2	93.58(5)	93.36(3)	88.52(3)	90.59(3)	116.36(15)	97.12(7) and 98.72(7)
N−Zr−X[d]	90.11(7)−97.54(7)	90.07(5)−95.48(4)	83.53(6)−92.51(7)	88.95(7)−91.41(7)	78.34(13)−94.59(12)	87.78(7)−102.55(8)

[a] Atom numeration according to **3a**. Values were provided for analogous atoms in other structures, *independent of the numeration in the respective complex*. [b] Nitrogen atoms *trans* to Cl, numeration differs between complexes. [c] Nitrogen atoms *trans* to N, numeration differs between complexes. [d] X = Cl (**3a**−**c**), C (**5**), O (**6**). [e] Angle(s) between the least-squares planes defined by N1,N2,C2−C4 and Zr1,N1,N2 in **3a** or respective atoms in other complexes. [f] *cis*-angle(s) between nitrogen atoms of the same ligand. [g] *cis*-angle(s) between nitrogen atoms of different ligands.

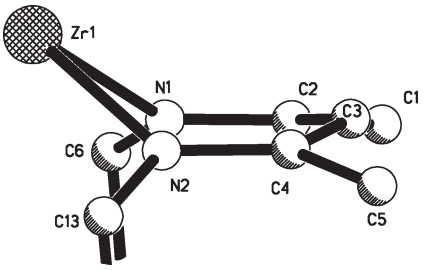

Figure 3. Boat-like conformation of the diketiminate ligand in **3a**.

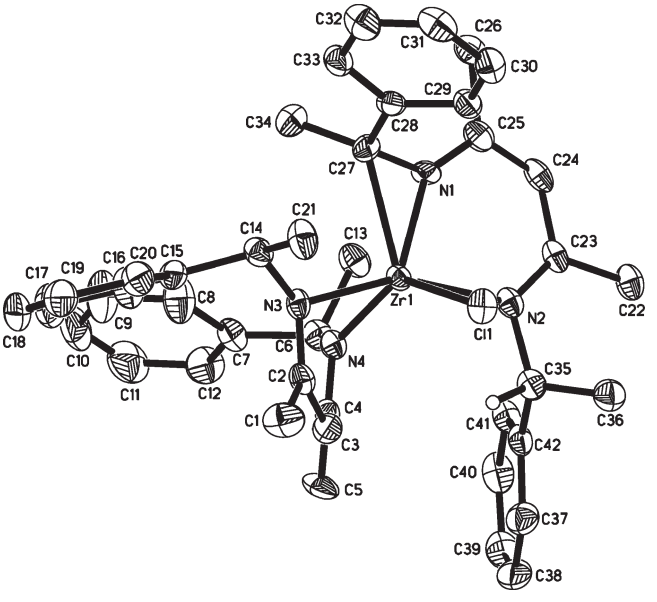

Figure 4. Crystal structure of complex **4** with 50% probability thermal ellipsoids depicted. Hydrogen atoms, other than H35, are omitted for clarity.

between Δ- and Λ-enantiomers, but not between *cis*- and *trans*-isomers. The isomerization is even slower in **3c**. Resonances in the ^{1}H and ^{13}C spectra are broadened by exchange, but show the presence of two diastereomeric complexes. Cooling of a $CDCl_3$ solution below 0 °C resulted in two signal sets in a 2:1 ratio for Δ-(*R*,*R*-*nacnac*^{MeBn})$ZrCl_2$, Δ-**3c**, and Λ-(*R*,*R*-*nacnac*^{MeBn})$ZrCl_2$, Λ-**3c**. A spectrum in the fast exchange region was not obtained in $CDCl_3$ or even in toluene-d_8 at

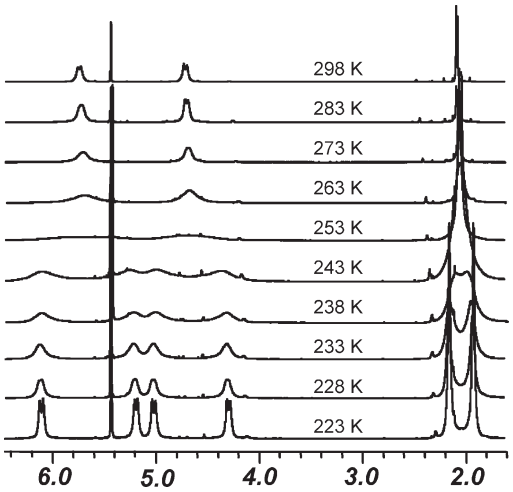

Figure 5. Variable-temperature ^{1}H NMR spectra of **3a**.

Table 2. Selected Bond Distances [Å] and Bond Angles [deg] for 4

Zr1−Cl1	2.477(1)	N1−C25	1.330(6)
Zr1−N1	2.031(3)	C24−C25	1.366(8)
Zr1−N2	2.318(4)	C23−C24	1.437(7)
Zr1−N3	2.230(3)	N2−C23	1.323(6)
Zr1−N4	2.196(4)	N1−Zr1−N2	76.6(2)
Zr1−C27	2.305(5)	N3−Zr1−N4	83.5(1)
N1−C27	1.410(7)	N1−Zr1−N4	109.1(2)

100 °C. In contrast to **3a** and **3b**, coalescence into a fully symmetric spectra requires two different Bailar-twists for **3c**. The mechanism depicted in Scheme 2 will exchange groups *trans* to N in the Δ-isomer (short: Δ-N, Scheme 3) with groups *trans* to Cl in the Λ-isomer (short: Λ-Cl). Since the pairs Δ-N/Λ-Cl and Λ-N/Δ-Cl are enantiomeric in **3a** and **3b**, only one resonance is observed for these groups. This is not the case for diastereomeric Δ-**3c** and Λ-**3c**, and a second Bailar-twist mechanism is required to exchange Δ-N with Δ-Cl (or Λ-N with Λ-Cl, respectively). Since this requires one diketiminate ligand to bridge the two trigonal faces of the prismatic transition state (Scheme 3), the latter is probably of higher energy.[23] The presence of two, eventually overlapping

(23) For **3a**, the second Bailar-twist would lead to an exchange of H_a and H_b (Scheme 2). That two doublets are observed for the diastereotopic CH_2 hydrogens of **3a** at room temperature is in agreement with a higher activation barrier for this isomerization.

Scheme 2

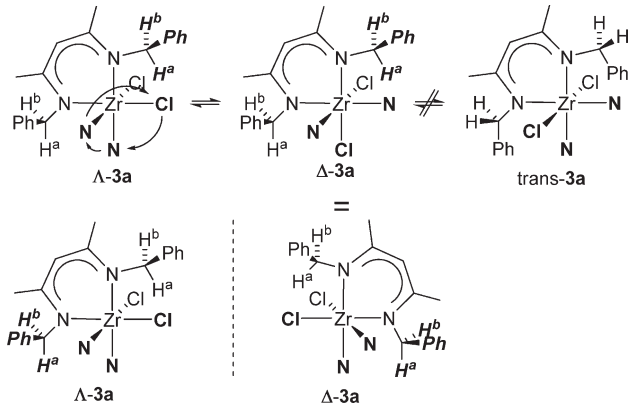

Scheme 3. Exchange of Δ-Cl First with Λ-N, Then with Δ-N

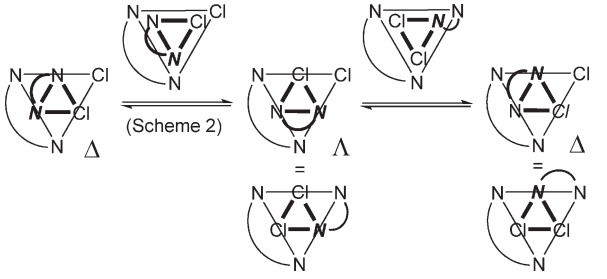

Table 3. Activation Parameters Determined from Eyring Plots of k_{obs} for the Isomerization of *nacnac*$^{R}{}_2$ZrX$_2$[a]

complex	R/X	$\Delta H^{\ddagger}$ [kJ·mol^{-1}]	$\Delta S^{\ddagger}$ [J·mol^{-1}·K^{-1}]	k_{298K} [$\times 10^3$ s^{-1}]
3a	Bn/Cl	51(1)	18(3)	60
3b	Cy/Cl	48(2)	−27(9)	1
6	Bn/OEt	48(1)	−16(6)	3

[a] Temperature range used for determination of $\Delta H^{\ddagger}$ and $\Delta S^{\ddagger}$: 223−283 K (**3a**), 233−318 K (**3b**), 223−298 K (**6**).

exchange processes might explain the lack of coalescence even at higher temperatures. The presence of four C*H*(Me)Ph resonances in the ^{1}H NMR spectrum of **3c** at room temperature and two H*C*(=N)$_2$ resonances in its ^{13}C spectrum indicates that even the first Bailar-twist, which leads to Δ−Λ-isomerization, is slow on the NMR time scale at room temperature. Nevertheless, the chiral diketiminate complex **3c** does not have the configurational stability exhibited, for example, by the chiral "IAN amino" zirconium complexes of Johnston and co-workers,[3] since, in contrast to those, Δ−Λ-isomerization in **3c** does not require ligand enantiomerization.

Simulation of the line shape of selected peaks in the ^{1}H NMR spectra of **3a**−**c** allowed the determination of exchange rates (k_{obs}) at different temperatures (see Experimental Section) Activation parameters were obtained from Eyring plots of these rate constants (Figure 6, Table 3). While satisfactory linear plots and identical values from different pairs of exchanging nuclei were obtained for **3a** and **3b**, a smaller temperature window and difficulties in the determination of exchange constants made the determination rather unreliable for **3c**. Activation enthalpies for **3a** and **3b** (Table 3) are slightly higher than that of *nacnac*$^{Ph}{}_2$ZrCl$_2$ (38 kJ/mol),[6] but comparable to those in other *nac*(*n*)*ac*$_2$ZrX$_2$ complexes (36−57 kJ/mol),[7,12] which undergo the same

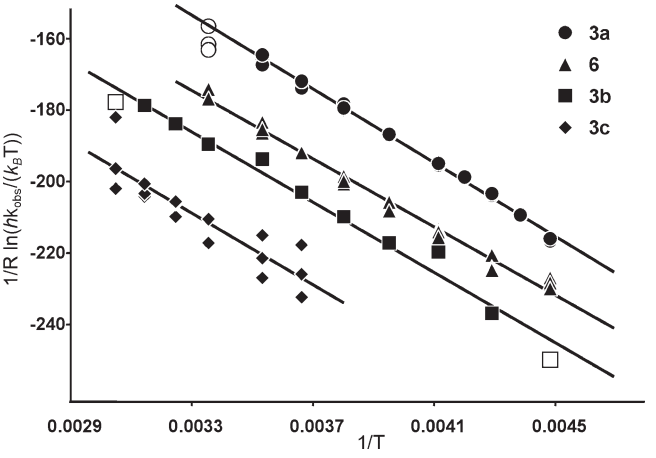

Figure 6. Eyring plots of the exchange rates for isomerizations of **3a**−**c** and **6** (hollow data points not used in linear regression analysis).

exchange process. The activation entropy of 18(3) J/(mol·K) for **3a** is significantly more positive than those previously observed (−39 to −56 J/(mol·K))[6,7,12] and might be indicative for a dissociation/recoordination mechanism instead of a Bailar-twist mechanism for **3a**. However, a negative activation entropy is obtained for **3b**, although its crystal structure indicates increased steric interactions in the presence of a cyclohexyl substituent on nitrogen, and **3b** would be expected to be even more prone to follow a dissociation/recoordination mechanism than **3a**. In addition, as will be discussed below, alkylation of **3a** can be aided by partial dissociation of diketimine. The inactivity of **3a**−**c** toward alkylation (*vide infra*) indicates that a five-coordinated intermediate is not present with sufficient lifetime to allow chloride−alkyl exchange. While a dissociation mechanism for **3a** can thus not be excluded, it seems incompatible with additional data. An alternative explanation would involve a less restricted rotation around the N−CH$_2$ bond in the prismatic transition state, which is blocked in the Δ/Λ-ground state. In agreement with this, the activation entropy obtained for **3b**, which has only one hydrogen on the secondary alkyl substituent and no other accessible rotamers, is comparable to those in *N*-aryl-substituted complexes.

***nacnac*$_2$ZrMe$_2$ Complexes.** Attempts to prepare alkyl derivatives of **3a**−**c** using alkylating agents such as MeLi, MeMgBr, BnMgBr, ZnEt$_2$, *t*BuLi, or *n*BuLi in a variety of solvents and reaction conditions did not meet with success. NMR spectra of reaction products showed only the presence of starting material or, under forcing conditions such as prolonged heating, decomposition products. Since alkylation seemed impossible after complexation of the *nacnac* ligand, we decided to introduce the methyl group prior to complexation.[24] Indeed, the dimethyl analogue **5** was obtained in moderate yield (60%) by reaction of ZrCl$_4$ first with 2 equiv of MeLi and then with the lithium salt **2a** (Scheme 4). Only **5** was accessible by this pathway. As observed for the synthesis of the dichloride complexes, ligands with secondary alkyls on N, i.e., **2b** and **2c**, did not react fast enough to compete with the decomposition of the zirconium alkyl chloride complex.

(24) Park, J. T.; Woo, B. W.; Yoon, S. C.; Shim, S. C. *J. Organomet. Chem.* **1997**, *535*, 29.

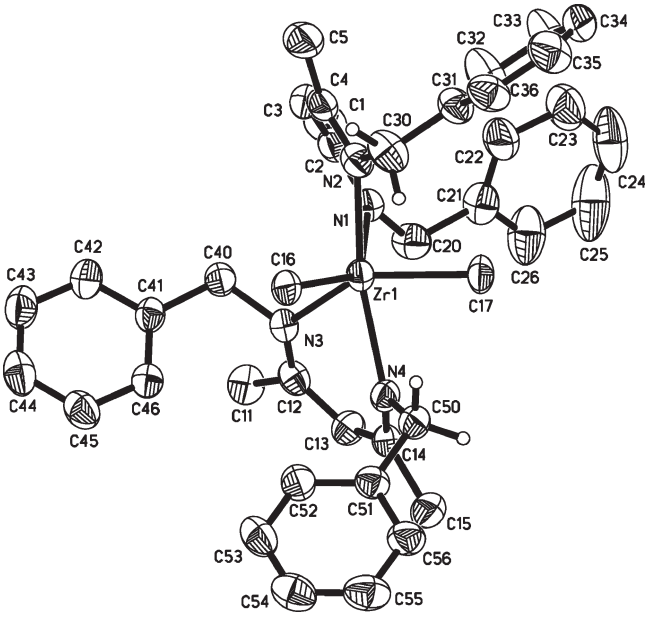

Figure 7. Crystal structure of complex **5**. Thermal ellipsoids are drawn at the 50% probability level, and most H atoms are omitted for clarity.

Scheme 4

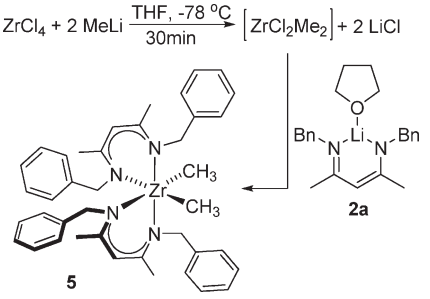

The solid-state structure of **5** shows the octahedral *cis*-geometry previously observed (Figure 7), but with a significantly more pronounced deviation from ideal geometry (N−Zr−N/X angles of 75−127°), while the bending angle of 31° is the smallest observed (Table 1). A possible reason for the increased deviation might lie in the shorter Zr−Me distance in **5** (2.290(4) and 2.297(4) Å), when compared to Zr−Cl in **3a** (2.454(1) Å). The closer distance to the benzyl CH_2 group (C30 and C50, Figure 7) results in a widening of the X−Zr−X angle by 23° (**3a**, Cl1−Zr1−Cl1: 93.6(1)°; **5**, C16−Zr1−C17: 116.4(2)°) and subsequent distortion of the octahedral geometry.

Reactions of styrene with **3a**−**c**/$AlCl_{3-x}Me_x$ (x = 1−3),[25] **3a**/$AlMe_3$/H_2O,[26] **5**/$AlCl_{3-x}Me_x$ (x = 0−3), or **5**/$B(C_6F_5)_3$,[27] in polar or apolar solvents, at room temperature or upon heating, showed no evidence for insertion of the olefin into the Zr−Me bond (NMR, GC-MS). No insertion was likewise observed in reactions of **5**/$B(C_6F_5)_3$ with diphenylacetylene

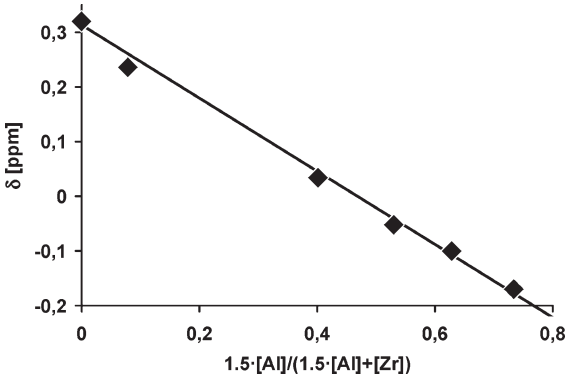

Figure 8. Chemical displacement of the averaged methyl resonance in **5**/$AlMe_3$ mixtures in C_6D_6.

Scheme 5

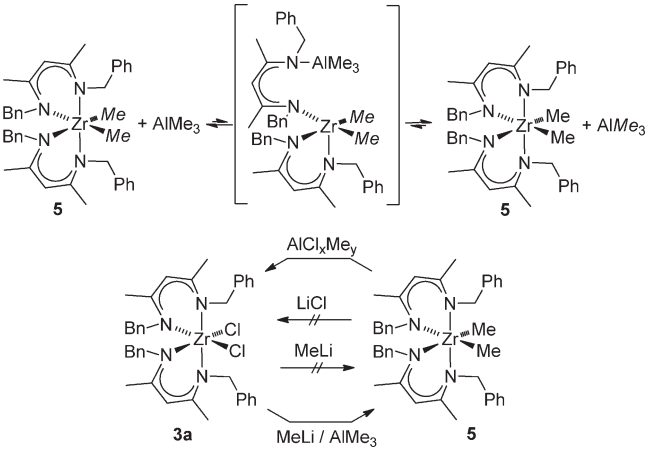

or benzaldehyde. Surprisingly with regard to the failed attempts to exchange chloride against alkyl ligands, **5** reacted fast with $AlCl_{3-x}Me_x$ (x = 0−2) in C_6D_6 solution to yield the dichloride complex **3a**. To investigate this further, a C_6D_6 solution of **5** was titrated with $AlMe_3$ (0−1.8 equiv). ^{1}H NMR spectra, recorded after each addition, showed no change in the diketiminate ligand resonances, but only one averaged resonance for Zr- as well as Al-bound methyl groups, which shifted from 0.32 (Al/Zr = 0) to −0.23 ppm (Al/Zr = 1.8) as the concentration of $AlMe_3$ increased (Figure 8). Interpolation of the linear regression line yielded a reasonable value of δ −0.36 ppm for pure $AlMe_3$ in C_6D_6. Exchange of methyl groups between Al and Zr centers is thus occurring fast on the NMR time scale, in contradiction with the problems encountered in the alkylation of these complexes. This might indicate that alkylation of **3a**−**c** is a thermodynamic, rather than a kinetic, problem. Alternatively, interaction of $AlMe_3$ with a diketiminate ligand might loosen its coordination to zirconium, rendering the methyl ligands in **5** more accessible for exchange processes (Scheme 5). Additional experiments support the latter explanation: Reaction of C_6D_6 solutions of **5** with excess LiCl did not lead to the formation of the dichloride complex **3a**, and methyl against chloride exchange is thus no more feasible than chloride against methyl.[28] On the other hand, when C_6D_6 solutions of the dichloride complex **3a** were reacted with

(25) Kondakov, D. Y.; Negishi, E. *J. Am. Chem. Soc.* **1996**, *118*, 1577.
(26) Wipf, P.; Ribe, S. *Org. Lett.* **2000**, *2*, 1713.
(27) Reaction of **5** with $B(C_6F_5)_3$ in C_6D_6 solution yielded NMR spectra in agreement with the formation of the ion pair $[(nacnac^{Bn})_2ZrMe][MeB(C_6F_5)_3]$: only one peak each is observed for all CH_2, CH, or Me groups of the diketiminate ligands in ^{1}H and ^{13}C spectra, while the former $ZrMe_2$ group splits into two signals. The ion-pair is only metastable in solution and rapidly separates as a red oil.

(28) Minor amounts of **3a** (ca. 5%) were attributed to the presence of traces of water and excess LiCl. These amounts increased if aged LiCl, not kept from moisture, is used.

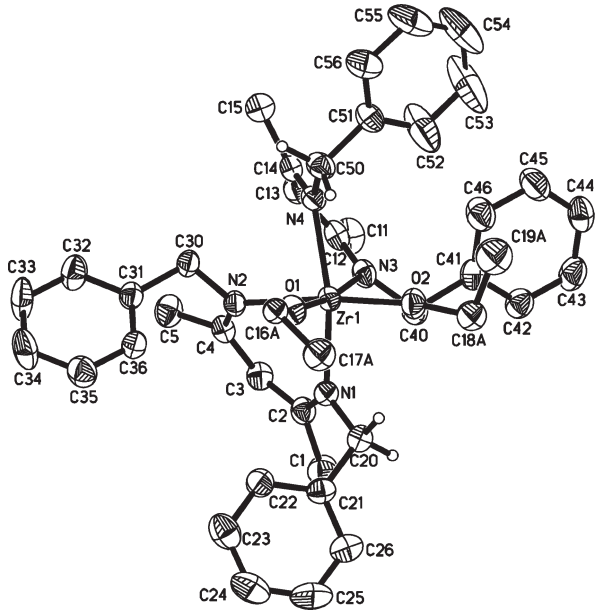

Figure 9. Crystal structure of **6**. Only one of two independent molecules is shown. Thermal ellipsoids are drawn at the 50% probability level. The minor occupied positions of the disordered ethyl groups and most H atoms are omitted for clarity.

methyllithium in the presence of 10 equiv of $AlMe_3$, the obtained reaction mixtures contained up to 90% of the dimethyl complex **5** (Scheme 5). Ligand exchange between **3a** and **5** is thus most likely aided by a loosening of the diketiminate coordination with $AlMe_3$.

While **3a** did not undergo ligand exchange with NaOEt, reaction of **5** with 2 equiv of ethanol afforded the dialkoxide complex *nacnac*$^{Bn}{}_2$Zr(OEt)$_2$, **6**.[29] Despite Zr−O distances even shorter (1.939(2)−1.954(2) Å) than Zr−Me in **5** (2.290(4) and 2.297(4) Å), its crystal structure (Figure 9) is again very similar to that of the dichloride complex **3a**, with O−Zr−O angles of 97.12(7)° and 98.72(7)° and a slightly distorted octahedral coordination environment (Table 1). This might be related to the smaller vdW radius of oxygen compared to chloride and methyl, which can accommodate a shorter Zr−O distance: shortest distances between a benzyl hydrogen and the Zr−X ligand (**3a**, *d*(H−Cl) = 2.9 Å; **5**, *d*(H−C) = 2.8 Å; **6**, *d*(H−O) = 2.5 Å) are in all three complexes only slightly shorter than the sum of their vdW radii (H−Cl: 3.0 Å, H−C: 2.9 Å, H−O: 2.7 Å). Again, a fluxional process was observed by NMR. In addition to the changes observed for **3a** and **5**, the quartet of the CH_2O group splits into two multiplets of equal intensity at −50 °C, confirming again that the fluxional process is associated with a racemization of the complex. Activation parameters yielded an activation enthalpy comparable to **3a**, but an activation entropy lower by 34 J/(mol·K) ($\Delta S^{\ddagger} = -16(6)$ J/(mol·K), Table 3), which might indicate reduced rotational freedom of the ethoxy substituents in the transition state.

Conclusions

While not accessible with *ortho*-substituted *N*-aryl diketiminate ligands, *β*-diketiminates with aliphatic *N*-alkyl substituents readily form bis(diketiminate) zirconium complexes, even with bulky secondary alkyls, and offer access to an easy modification of the steric environment. Steric crowding caused by the N-substituent seems the most likely cause for the inactivity of the dichloride complexes toward ligand exchange. It does not impede fast complex racemization, however, most probably by a Bailar-twist mechanism. While structural analyses confirm the targeted proximity of the alkyl substituent and the reactive coordination sites and the potential utility of the ligand framework in catalysis, the dimethyl complex **5** does not insert styrene, diphenylacetylene, or benzaldehyde when activated with $AlMe_{3-x}Cl_x$ or $B(C_6F_5)_3$, which might be due again to steric crowding or a too low Lewis acidity of the metal center. Complex racemization proved to be too fast to impart selectivity in lactide polymerizations. We are currently investigating the effects of interligand bridging to control complex racemization and to improve the reactivity of this class of compounds.

Experimental Section

All reactions, except ligand synthesis, were carried out under an inert atmosphere using Schlenk and glovebox techniques under a nitrogen atmosphere. *nacnac*^{Bn}H (**1a**),[18] *R,R-nacnac*^{MeBn}H (**1c**),[17] and $ZrCl_4(THF)_2$[30] were prepared according to literature procedures. All other chemicals were purchased from common commercial suppliers and used without further purification. THF was distilled from sodium/benzophenone; all others solvents were dried by passage through activated aluminum oxide (MBrown SPS) and deoxygenated by repeated extraction with nitrogen. C_6D_6 was dried over sodium, $CDCl_3$ was dried over CaH_2, and both were distilled under reduced pressure and then degassed by three freeze−pump−thaw cycles. Styrene and ethanol were evacuated under vacuum and dried over 4 Å molecular sieves. ^{1}H and ^{13}C NMR spectra were acquired on a Bruker AMX 300 or Bruker AV 400 spectrometer. ^{19}F NMR spectra were acquired on a Bruker Avance 300. Chemical shifts were referenced to the residual signals of the deuterated solvents (C_6D_6: ^{1}H: *δ* 7.16 ppm, ^{13}C: *δ* 128.38 ppm; $CDCl_3$: ^{1}H: *δ* 7.26 ppm, ^{13}C: *δ* 77.00 ppm; C_7D_8: ^{1}H: *δ* 2.09 ppm, ^{13}C: *δ* 20.40 ppm). Low-temperature NMR spectra were recorded using a Bruker AV 500 spectrometer. NMR data at low or high temperatures are given in the Supporting Information. Exchange rates were obtained by comparison of experimental and simulated spectra with the WINDNMR program.[31] Elemental analyses were performed by the Laboratoire d'Analyse Élémentaire (Université de Montréal).

2-Cyclohexylamino-4-cyclohexyliminopent-2-ene, *nacnac*^{Cy}H, 1b.[19] Acetylacetone (1.00 g, 10 mmol), *para*-toluenesulfonic acid monohydrate (1.9 g, 10 mmol), and cyclohexylamine (1.0 g, 10 mmol) were combined with toluene (100 mL). The resulting white suspension was refluxed for 3 h with the help of Dean−Stark apparatus to afford a colorless solution. After cooling to room temperature, a second equivalent of cyclohexylamine (1.0 g, 10 mmol) was added and the reaction mixture was refluxed for 3 days. A colorless precipitate appeared upon cooling to room temperature, which was separated by filtration and combined with 100 mL of ether and 100 mL of an aqueous solution of KOH (5.6 g, 100 mmol). Phases were separated and the aqueous phase was extracted with ether. The combined phases were dried over Na_2SO_4 and filtered, and the solvent was evaporated. The obtained yellow liquid was allowed to cool slowly to room temperature to yield colorless crystals (1.8 g, 69%). The crude product contained ca. 5% impurities according to NMR, but was used without further purification in subsequent reactions. Recrystallization from ethanol afforded analytically pure compound.

(29) Complex **6** can be employed as initiator for the polymerization of *rac*-lactide in molten monomer (Zr/lactide = 1:200, 130 °C, 98% conversion in 0.5 h), but yielded essentially atactic polymer (P_r = 0.6).

(30) Manzer, L. E. *Inorg. Synth.* **1982**, *21*, 135.
(31) Reich, H. J. *WinDNMR*; J. Chem. Educ. Software 3D2, **1996**.

^{1}H NMR ($CDCl_3$, 400 MHz, 298 K): δ 11. 72 (bs, 1H, NH), 4.44 (s, 1H, CH(C=N)$_2$), 3.32−3.35 (m, 2H,CH(Cy)), 1.90 (s, 6H, Me(C=N)), 1.80−1.35 (m, 20H, Cy). ^{13}C{^{1}H} NMR ($CDCl_3$, 101 MHz, 298 K): δ 158.4 (*C*=N), 93.7(*C*H(C=N)$_2$), 54.1 (*C*H$_{Cy}$), 34.6 (*C*H$_{2a}$), 25.7 (*C*H$_{2b}$), 25.7 (*C*H$_{2c}$), 18.8 (*C*H$_3$). Anal. Calcd for $C_{17}H_{30}N_2$: C, 77.80; H, 11.52; N, 10.62. Found: C, 77.60; H, 11.24; N, 10.85.

***Nacnac*^{Bn}Li(THF), 2a.** A hexane solution of *n*BuLi (1.36 mL, 2.9 M, 3.95 mmol) was added over 25 min at room temperature to a yellow THF solution of **1a** (1.0 g, 3.6 mmol). The yellow-orange solution was allowed to stir for 4 h. The volatiles were removed, and the remaining solid was washed with 2 × 5 mL of hexane. The solid was dried under reduced pressure to yield a colorless powder (1.25 g, 90%) and used without further purification.

^{1}H NMR ($CDCl_3$, 400 MHz): δ 7.22−7.30 (m, 10H, Ph), 4.54 (s, 1H, C*H*(C=N)$_2$), 4.42 (s, 4H, C*H*$_2$Ph), 3.74 (m, 4H, THF), 1.93 (s, 6H, *Me*(C=N)), 1.83 (m, 4H, THF). ^{1}H NMR (C_6D_6, 400 MHz): δ 7.00−7.30 (m, 10H, Ph), 4.82 (s, 1H, C*H*(C=N)$_2$), 4.60 (s, 4H, C*H*$_2$Ph), 2.86 (m, 4H, THF), 2.09 (s, 6H, *Me*-(C=N)), 0.98 (m, 4H, THF). ^{13}C{^{1}H} NMR ($CDCl_3$, 101 MHz): δ 161.0 (C=N), 140.9 (*ipso* Ph) 128.3 (*ortho* Ph), 127.2 (*para* Ph), 126 (*meta* Ph), 95.1 (*C*H(C=N)$_2$), 67.9 (THF), 50.7 (*C*H$_2$(Ph)), 25.6 (THF), 19.6 (*Me*(C=N)). ^{13}C{^{1}H} NMR (C_6D_6, 101 MHz): δ 165.8 (C=N), 145.4 (*ipso* Ph) 128.5 (*ortho* Ph), 127.5 (*para* Ph), 126.0 (*meta* Ph), 93.8 (*C*H(C=N)$_2$), 67.5 (THF), 50.7 (*C*H$_2$(Ph)), 25.1 (THF), 22.0 (*Me*(C=N)).

***nacnac*^{Cy}Li(THF), 2b.** To a yellow THF solution of **1b** (1.5 g, 5.8 mmol) was added gradually a hexane solution of *n*BuLi (2 mL, 2.9 M, 5.8 mmol) at room temperature. After 4 h of stirring the solution turned orange. The volatiles were removed under reduced pressure to yield **2b** as a yellow solid (1.9 g, 96%), which was used without further purification.

^{1}H NMR (C_6D_6, 400 MHz, 298 K): δ 4.56 (s, 1H, C*H*(C=N)$_2$), 3.40−3.44 (m, 6H, Cy C*H* and C*H*$_2$O), 2.16 (s, 6H, C*H*$_3$), 1.77−1.3 (m, 24H, THF and Cy C*H*$_2$). ^{13}C{^{1}H} NMR (C_6D_6, 101 MHz, 298 K): δ 158.0 (*C*=N), 95.0 (*C*H(C=N)$_2$), 54.6 (THF), 54.4 (Cy *C*H), 34.6 (*C*H$_{2a}$), 25.7 (*C*H$_{2b}$), 25.7 (*C*H$_{2c}$), 24.5 (THF), 18.8 (*C*H$_3$).

***R,R-nacnac*^{MeBn}Li(THF), 2c.** A solution of *n*BuLi in hexane (2.9 M, 0.9 mmol) was added gradually over 10 min to a yellow THF solution of **1c** (0.25 g, 0.82 mmol). The yellow-orange solution was allowed to stir for 4 h at room temperature, volatiles were evaporated, and a brown oil was obtained (0.30 g, 92%), which was used without further purification.

^{1}H NMR (400 MHz, C_6D_6): δ 7.16−7.42 (m, 10H, *Ph*), 4.81 (q, 2H, *J* = 7 Hz, C*H*(Me)Ph), 4.71 (s, 1H, C*H*(C=N)$_2$), 3.00 (m, 4H, THF), 2.07 (s, 6H, *Me*(C=N)), 1.44 (d, 6H, *J* = 7 Hz, CH(*Me*)Ph), 0.97 (m, 4H, THF). ^{13}C{^{1}H} NMR (C_6D_6, 101 MHz): δ 161.0 (C=N), 150.2 (*ipso* Ph), 128.4 (*ortho* Ph), 126.6 (*para* Ph), 125.8 (*meta* Ph), 93.7 (*C*H(C=N)$_2$), 67.6 (*C*H(Me)Ph), 57.2 (THF), 25.5 (THF), 24.6 (CH(*Me*)Ph), 22.3 (*Me*(C=N)).

***nacnac*^{Bn}$_2$ZrCl$_2$, 3a.** **Method A.** In a dry Schlenk tube, $ZrCl_4$ (0.34 g, 1.4 mmol) and **2a** (1.0 g, 2.8 mmol) were mixed. Toluene (10 mL) was added under stirring. After 24 h at room temperature, the obtained orange mixture was filtered. The yellow filtrate was concentrated to half its volume, and the desired product was precipitated by addition of 15 mL of hexane. The yellow precipitate was separated by filtration and dried at a vacuum line to yield **3a** (0.35 g, 0.50 mmol, 35%).

Method B. A hexane solution of *n*BuLi (2.9 M, 5.4 mmol) was added to a toluene suspension of $ZrCl_4$ (0.62 g, 2.7 mmol) at −78 °C. The mixture was allowed to warm to room temperature and then stirred for another 12 h. To the obtained brown mixture was gradually added 15 mL of a toluene solution of **1a** (5.4 mmol, 1.5 g). The mixture was stirred for 2 days at 90 °C, during which it turned yellow. After cooling to room temperature, 20 mL of dichloromethane was added and the mixture was filtered. The combined volatiles were removed under vacuum, yielding **3a** as a yellow powder (1.5 g, 75%). Crystals suitable for X-ray diffraction studies were obtained by slow diffusion of hexane into a THF solution of the complex at 25 °C.

^{1}H NMR ($CDCl_3$, 400 MHz, 298 K): δ 7.20−7.30 (m, 20H, Ph), 5.65 (bs, 2H, C*H*$_2$Ph), 5.62 (bs, 2H, C*H*$_2$Ph), 5.32 (s, 2H, C*H*(C=N)$_2$), 4.61 (bs, 2H, C*H*$_2$Ph), 4.56 (bs, 2H, C*H*$_2$Ph), 1.92 (s, 12H, *Me*(C=N)). ^{13}C{^{1}H} NMR ($CDCl_3$, 101 MHz, 298 K): δ 167.1 (C=N), 139.5 (*ipso* Ph), 128.2 (*ortho* Ph), 127.2 (*para* Ph), 126.5 (*meta* Ph), 108.1 (*C*H(C=N)$_2$), 54.9 (*C*H$_2$Ph), 23.2 (*Me*(C=N)). Anal. Calcd for $C_{38}H_{42}ZrN_4Cl_2$: C, 63.66; H, 5.91; N, 7.82. Found: C, 63.00; H, 6.19; N, 7.69.

***nacnac*^{Cy}$_2$ZrCl$_2$, 3b.** In a dry Schlenk, $ZrCl_4$ (0.34 g, 1.5 mmol) and **2b** (1.0 g, 3.0 mmol) were mixed and toluene (10 mL) was added under stirring. After 24 h of stirring at room temperature the obtained orange mixture was filtered. The red filtrate was concentrated to half its volume, and the desired product was precipitated by addition of 15 mL of hexane. The white precipitate separated by filtration was dried at a vacuum line to yield **3b** (0.35 g, 35%). Crystals suitable for X-ray diffraction studies were obtained by slow diffusion of hexane into a THF solution of the complex at 25 °C.

^{1}H NMR ($CDCl_3$, 500 MHz, 298 K): δ 5.15 (s, 2H, C*H*-(C=N)$_2$), 4.25 (bm, 4H, Cy C*H*), 1.91 (bs, 12H, CH_3), 2.16−1.19 (m, 40H, Cy CH_2). ^{13}C{^{1}H} NMR ($CDCl_3$, 75 MHz, 298 K): Peaks severely broadened. For low- and high-temperature spectra see the Supporting Information Anal. Calcd for $C_{34}H_{58}ZrN_4Cl_2$: C, 59.62; H, 8.53; N, 8.18. Found: C, 58.98; H, 8.75; N, 7.71.

***R,R-nacnac*^{MeBn}$_2$ZrCl$_2$, 3c.** To a mixture of $ZrCl_4(THF)_2$ (0.77 g, 2.04 mmol) and **2c** (1.57 g, 4.08 mmol) was added toluene under stirring. The obtained orange mixture was allowed to react for 3 days at room temperature. The mixture was filtered, the orange filtrate concentrated to half its volume, and the desired product precipitated by addition of 15 mL of hexane. Recrystallization by slow diffusion of hexane into a saturated toluene solution gave yellow crystals of **3c** (1.1 g, 65%), contaminated with isolated red crystals of **4** (insufficient quantity for full characterization), which were separated by hand.

^{1}H NMR ($CDCl_3$, 400 MHz, 298 K) (peaks severely broadened; for low-temperature spectra of both diastereomers, see Supporting Information): δ 7.08−7.4 (m, 20H, *Ph*), 6.74 (bm, 2H, *b* C*H*(Me)Ph), 6.64 (bm, 2H, *a* C*H*(Me)Ph), 6.14 (bm, 2H, *a* C*H*(Me)Ph), 5.26 (bs, *a*+*b* C*H*(C=N)$_2$), 4.48 (bm, 2H, *b* C*H*-(Me)Ph), 2.15−1.63 (m, 24H, Me). ^{13}C{^{1}H} NMR ($CDCl_3$, 75 MHz, 298 K) (peaks severely broadened, many not observed or overlapping; for low-temperature spectra of both diastereomers, see Supporting Information): δ 168.1 (C=N), 167 (C=N), 162.9 (C=N), 143.9 (*ipso* Ph), 143.4 (*ipso* Ph), 110.8 (*C*H-(C=N)$_2$), 104.3 (*C*H(C=N)$_2$), 62 (*C*H(Me)Ph), 59.4 (*C*H(Me)-Ph), 57.6 (*C*H(Me)Ph), 27.2 (CH(*Me*)Ph), 25.3 (CH(*Me*)Ph), 19.8 (*Me*(C=N)), 18.2 (*Me*(C=N)), 17 (*Me*(C=N)). Anal. Calcd for $C_{42}H_{50}N_2ZrCl_2$: C, 65.26; H, 6.52; N, 7.01. Found: C, 64.93; H, 6.70 ; N, 7.13.

***nacnac*^{Bn}$_2$ZrMe$_2$, 5.** $ZrCl_4$ (0.42 g, 1.8 mmol) was dissolved in THF (60 mL). An ether solution of MeLi (2.5 mL, 1.6 M, 4.0 mmol) was added at −78 °C under exclusion of light. The obtained white suspension was allowed to stir for 30 min in order to generate Me_2ZrCl_2. To the obtained mixture was added **2a** (1.28 g, 3.6 mmol), affording a yellow suspension. The mixture was allowed to warm to room temperature during 18 h, upon which it turned red. The volatiles were evaporated under reduced pressure to give an orange solid film. The product was extracted with CH_2Cl_2 (20 mL), and the resulting red solution was evaporated to dryness to yield **5** as a yellow powder (0.70 g, 63%). Crystals suitable for X-ray diffraction analysis were obtained by slow diffusion of hexane into a saturated toluene solution at −20 °C.

^{1}H NMR (C_6D_6, 400 MHz, 298 K): δ 7.60−7.06 (m, 20H, Ph), 4.94 (s, 2H, CH(C=N)$_2$), 4.77 (bs, 8H, CH_2), 1.76 (s, 12H, Me(C=N)), 0.32 (s, 6H, Me-Zr). ^{13}C{^{1}H} NMR (C_6D_6, 101

Table 4. Details of X-ray Diffraction Studies

	3a	3b	3c	4	5	6
formula	$C_{38}H_{42}Cl_2N_4Zr$	$C_{34}H_{58}Cl_2N_4Zr$	$C_{42}H_{50}Cl_2N_4Zr$	$C_{42}H_{49}ClN_4Zr$	$C_{40}H_{48}N_4Zr$	$C_{42}H_{52}N_4O_2Zr$
M_w (g/mol); $F(000)$	716.88; 1488	684.96; 1456	772.98; 1616	736.52; 772	676.04; 1424	736.10; 3104
cryst color and form	yellow block	colorless block	yellow fragment	red plate	yellow plate	colorless plate
cryst size (mm)	0.12 × 0.06 × 0.03	0.60 × 0.28 × 0.10	0.10 × 0.08 × 0.04	0.06 × 0.06 × 0.04	0.06 × 0.05 × 0.02	0.06 × 0.04 × 0.02
T (K); wavelength	200; 0.71073	150; 1.54178	150; 1.54178	150; 1.54178	150; 1.54178	150; 1.54178
cryst syst	tetragonal	monoclinic	monoclinic	monoclinic	monoclinic	orthorhombic
space group	$P4_32_12$	$C2/c$	$P2_1$	$P2_1$	$P2_1/n$	$P2_12_12_1$
unit cell: a (Å)	8.7244(5)	20.2320(8)	13.6460(3)	13.5011(18)	15.2045(13)	11.6079(9)
b (Å)	8.7244(5)	9.0276(4)	20.5189(5)	9.1289(11)	9.6321(8)	15.7760(12)
c (Å)	47.453(6)	22.539(1)	14.4588(4)	15.1108(18)	24.0981(19)	42.516(3)
β (deg)	90	91.250(2)	108.891(1)	95.413(7)	97.213(4)	90
V (Å^3); Z; $d_{calcd.}$ (g/cm^3)	3611.9(6); 4;1.318	4115.7(3); 4; 1.105[a]	3830.41(16);4; 1.340	1854.1(4); 2; 1.319	3501.3(5); 4; 1.283	7785.8(10); 8; 1.256
θ range (deg); completeness	1.7−27.6; 1.0	3.9−72.3; 0.99	3.2−58.0; 0.99	2.9−68.1; 0.98	3.3−67.5; 1.0	2.1−67.9; 1.0
collected reflns; R_σ	99 235; 0.070	53 603; 0.021	60 497; 0.025	27 516; 0.082	54 484; 0.063	137 856; 0.027
unique reflns; R_{int}	4177; 0.144	4013; 0.036	10 532; 0.046	6510; 0.079	6282; 0.116	14 075; 0.060
μ (mm^{-1}); abs corr	0.484; multiscan	3.554; multiscan	3.893; multiscan	3.348; multiscan	2.813; multiscan	2.611; multiscan
R1(F); wR(F^2) ($I > 2\sigma(I)$)	0.039; 0.069	0.034; 0.098	0.025; 0.064	0.050; 0.127	0.045; 0.101	0.027; 0.072
R1(F); wR(F^2) (all data)	0.075; 0.078	0.034; 0.098	0.027; 0.065	0.058; 0.131	0.076; 0.117	0.029; 0.073
GoF(F^2)	0.920	1.113	1.029	0.793	1.013	1.026
residual electron density (e$^-$/Å^3)	0.28	0.40	0.53	1.28	0.88	0.31

[a] Co-crystallized solvent removed with SQUEEZE.

MHz, 298 K): δ 163.5 (C=N), 140.2 (*ipso* Ph), 128.1 (*ortho* Ph), 126.6 (*para* Ph), 126.1 (*meta* Ph), 100.5 (*C*H(C=N)), 52.1 (*C*H$_2$Ph), 41.2 (Me-Zr), 21.4 (*Me*(C=N)). Anal. Calcd for $C_{40}H_{48}N_4Zr$: C, 71.06; H, 7.16; N, 8.29. Found: C, 71.59; H, 7.28; N, 8.29.

Reaction of 5 with B(C$_6$F$_5$)$_3$. To a C_6D_6 solution of B(C$_6$F$_5$)$_3$ (7.5 mg, 0.0148 mmol) in a J. Young NMR tube was added 0.5 mL of a yellow C_6D_6 solution of **5** (2.96×10^{-3} M, 0.0148 mmol) in portions of 0.1 mL every 5 min to give [*nacnac*$^{Bn}_2$ZrMe][MeB(C$_6$F$_5$)$_3$]. A red oil separated from the solution upon standing.

^{1}H NMR (C_6D_6, 400 MHz, 298 K): δ 7.37−7.06 (m, 20H, Ph), 4.89 (bs, 2H, CH(C=N)$_2$), 4.54 (bs, 8H, CH$_2$), 1.77 (bs, 12H, Me(C=N)), 0.43 (s, 3H, MeB), 0.19 (s, 3H, MeZr). ^{13}C{^{1}H} NMR (C_6D_6, 101 MHz, 298 K): δ 191.0 (C=N), 136.9 (*ipso* Ph), 129.3 (B(C$_6$F$_5$)$_3$) 128.3 (B(C$_6$F$_5$)$_3$), 128.1 (*ortho* Ph), 128.05 (*para* Ph), 127.9 (*meta* Ph), 126.9 (B(C$_6$F$_5$)$_3$), 93.2 (*C*H(C=N)), 31.9 (*C*H$_2$Ph), 23.0 (MeB), 21.4 (*Me*(C=N)), 14.4 (MeZr).

***nacnac*$^{Bn}_2$Zr(OEt)$_2$, 6.** Ethanol (37.5 mg, 0.81 mmol) was added to a yellow ether solution of **5** (250 mg, 0.37 mmol), upon which gas formation (CH$_4$) was observed. The yellow solution was evaporated to dryness, and the obtained yellow solid was extracted with 15 mL of hexane. Evaporation of the volatiles yielded a colorless powder, which contained mostly **6** and the free ligand **1a**. Recrystallization from a saturated ethanol solution at −20 °C gave colorless crystals of **6** (136 mg, 50%).

^{1}H NMR ($CDCl_3$, 400 MHz, 298 K): δ 7.30−7.06 (m, 20H, Ph), 5.10 (bs, 4H, CH$_2$), 4.86 (s, 2H, CH(C=N)$_2$), 4.54 (bs, 4H, CH$_2$), 3.69 (q, 4H, CH$_2$O), 1.83 (bs, 12H, Me(C=N)), 0.72 (t, 6H, *Me*CH$_2$O). ^{13}C{^{1}H} NMR (C_6D_6, 400 MHz, 298 K): δ 163.5 (C=N), 142.1 (*ipso* Ph), 127.9 (*ortho* Ph), 127.2 (*para* Ph), 125.8 (*meta* Ph), 102.7 (*C*H(C=N)), 64.7 (CH$_2$O), 53.6 (*C*H$_2$Ph), 22.2 (*Me*CH$_2$O), 19.8 (*Me*(C=N)). Anal. Calcd for $C_{42}H_{48}N_4O_2Zr$: C, 68.53; H, 7.12; N, 7.61. Found: C, 68.13; H, 7.45; N, 7.68.

Variable-Temperature NMR Measurements. Variable-temperature NMR spectra were recorded using a Bruker AV 500 spectrometer with $CDCl_3$ solutions of complexes **3a**−**c** and **6**. NMR data at low or high temperatures are given in the Supporting Information. Exchange rates were obtained by simulation of the experimental spectra with the WINDNMR program.[31] Temperature range, exchange simulated: **3a**, 223−298 K, *Me*(CN) and both diastereotopic NC*H*$_2$Ph; **3b**, 223−328 K, N−C*H*=(CH$_2$)$_5$; **3c**, 223−328 K, *Me*(CN) and both diastereotopic C*H*(Me)Ph; **6**, 223−298 K, *Me*(CN) and both diastereotopic MeC*H*$_2$O.

X-ray Diffraction Studies. Diffraction data for complexes **3a** were recorded on a Bruker Smart APEXII (Mo radiation) diffractometer, for complex **4** on a Bruker Smart 6000 (Cu rotating anode), and for all others on a Bruker Proteum X8/Microstar (Cu radiation), using the APEX2 software package.[32] Data reduction was performed with SAINT;[33] absorption corrections with SADABS.[34] Structures were solved with direct methods (SHELXS97).[35] All non-hydrogen atoms were refined anisotropically using full-matrix least-squares on F^2, and hydrogen atoms were refined with fixed isotropic U using a riding model (SHELXL97).[35] For **3b**, the cocrystallized solvent was identified as a disordered hexane (in agreement with NMR data), but could not be resolved and thus was suppressed by application of SQUEEZE.[36] For further details see Table 4 and the Supporting Information.

Acknowledgment. We thank Sylvie Bilodeau for variable-temperature NMR measurements and appreciate helpful discussions with Dr. Peter Burger and Dr. Marc-Heinrich Prosenc.

Supporting Information Available: Variable-temperature NMR data and crystallographic information files (CIF). This material is available free of charge via the Internet at http://pubs.acs.org.

(32) *APEX2*, Release 2.1-0; Bruker AXS Inc.: Madison, WI, 2006.
(33) *SAINT*, Release 7.34A; Bruker AXS Inc.: Madison, WI, 2006.
(34) Sheldrick, G. M. *SADABS*; Bruker AXS Inc.: Madison, WI, 1996 and 2004.
(35) Sheldrick, G. M. *Acta Crystallogr*. **2008**, *A64*, 112.
(36) Spek, A. L. *PLATON*; Utrecht University: Utrecht, The Netherlands, 2008.